Applied Physics Letters

RESEARCH ARTICLE | AUGUST 13 2026

Uncovering novel photoluminescence characteristics of Cu_2ZnSnS_4 thin-film solar cells through pulsed laser excitation

Jüri Krustok ; Achmad Nasyori ; Reelika Kaupmees ; Marit Kauk-Kuusik

Appl. Phys. Lett. 129, 062104 (2026)
https://doi.org/10.1063/5.0311985

AIP Publishing

Applied Physics Letters ARTICLE pubs.aip.org/aip/apl

Uncovering novel photoluminescence characteristics of Cu_2ZnSnS_4 thin-film solar cells through pulsed laser excitation

Cite as: Appl. Phys. Lett. **129**, 062104 (2026); doi: 10.1063/5.0311985
Submitted: 13 November 2025 · Accepted: 30 July 2026 ·
Published Online: 13 August 2026

Jüri Krustok,[a] Achmad Nasyori, Reelika Kaupmees, and Marit Kauk-Kuusik

AFFILIATIONS

Department of Materials and Environmental Technology, Tallinn University of Technology, Ehitajate tee 5, 19086 Tallinn, Estonia

[a]Author to whom correspondence should be addressed: juri.krustok@taltech.ee

ABSTRACT

Photoluminescence (PL) spectroscopy under pulsed laser excitation was employed to investigate the recombination mechanisms in a Cu_2ZnSnS_4 (CZTS) thin-film solar cell over a temperature range of 8–300 K. The PL spectra revealed one asymmetric band at 1.27 eV at T = 8 K, which was successfully fitted using an asymmetric double sigmoidal shape, indicating spatial variations in localized states and bandgap fluctuations. The PL band exhibited a temperature-dependent blue shift (∼0.26 meV/K) and low thermal activation energy (∼22 meV), suggesting recombination involving closely spaced deep donor–deep acceptor pairs. Laser power-dependent PL measurements at 8 K showed a pronounced blue shift of approximately 31 meV per decade of laser power, attributed to a band-filling effect under high excitation densities. The results support a model in which recombination occurs near band-bending regions. This study highlights the sensitivity of pulsed laser excitation PL, revealing previously unresolved recombination dynamics and localized states in CZTS-based photovoltaic materials.

The kesterite material Cu_2ZnSnS_4 (CZTS) has recently garnered significant attention as a promising solar cell absorber, owing to its appealing optical and electrical properties—such as a high absorption coefficient (∼10^4 cm^{-1}), inherent p-type conductivity, and an ideal bandgap (E_g ∼1.5–1.6 eV) for both single-junction photovoltaics and indoor photovoltaic applications. The highest reported power conversion efficiency of CZTS solar cells falls within the range of 11%–12%, which remains significantly below the Shockley–Queisser (SQ) theoretical limit of 32%.[1–5] One possible reason for this performance gap is the limited understanding of the various recombination processes, which contribute to the low current density and reduced open-circuit voltage observed in CZTS solar cells. Photoluminescence spectroscopy (PL) is widely recognized as a valuable tool for gaining insight into radiative recombination pathways in semiconductors. Typically, even at low temperatures, the PL spectra of CZTS exhibit a single wide asymmetric band at about 1.3 eV, which is attributed to band-to-defect or band-to-tail recombination.[6–10] In CZTS, a high concentration of charged intrinsic defects induces spatial potential fluctuations, which distort the valence and conduction band edges and result in the formation of exponential band tails in the density of states.[11] Moreover, it has been shown that spatial fluctuations in the bandgap energy can also produce similar tails. Bandgap fluctuations in CZTS are mainly caused by spatial distribution of ordered and disordered regions. In the ordered structure, Cu atoms occupy the 2a (0, 0, 0) and 2c (0, 1/2, 3/4) positions, while Zn atoms are located at the 2d (0, 1/2, and 1/4) position. However, in the disordered phase, Cu and Zn atoms are likely to be randomly distributed across the 2c and 2d positions, corresponding to the z = 1/4 and 3/4 planes.[8,12–14] The energy difference between the bandgaps (E_g) of these structures is approximately 100 meV, with the ordered structure exhibiting the higher E_g. Although T_C = 260 °C is determined to be the critical temperature at which the structure changes from an ordered to a disordered phase, the cooling rate has a significant impact on the degree of ordering.[8,15] It has been recognized that band tailing is a key factor contributing to the significant open-circuit voltage deficit currently limiting the performance of CZTS photovoltaic devices.[16] Potential fluctuations generally cause band tails with shapes that are close to exponential or Gaussian.[17] This results in asymmetric PL bands, where the low-energy side is partly governed by the shape of the band tails, while the steeper high-energy side is primarily influenced by electron–phonon interactions.[18,19] By analyzing the shape of the low-energy side, one can estimate the average depth of the potential fluctuations γ. It has

been demonstrated that the γ value in CZTS can reach as high as 50 meV.[20] The asymmetrical shape of CZTS PL bands is often fitted using asymmetric double sigmoidal (ADS) function.[21] However, the precise shape of PL bands in CZTS is influenced by multiple factors, including the shape of the band tails, variations in the bandgap energy arising from differing degrees of disorder, and the presence of certain defect clusters or grain boundaries. Specific defect clusters can induce deep and localized shifts in the conduction and valence band edges, thereby introducing extra recombination channels.[22,23] Additional recombination channels may also be formed near grain boundaries or dislocations as a result of band bending in the conduction and valence bands (see, for example, Ref. 24). The cliff-like band alignment of the CZTS/CdS heterojunction and interface defects in many CZTS solar cells encourage intense recombination at the interface.[25–27]

The majority of PL studies on CZTS have utilized continuous wave (CW) lasers as the excitation source. However, the use of a CW laser limits the maximum excitation density due to sample heating. To address this limitation, a pulsed laser with a pulse duration of less than 1 ns can be employed in conjunction with a synchronized lock-in detection system.[28] It was recently demonstrated that the use of pulsed laser excitation allows to expose various recombination mechanisms that are not typically observed with CW laser excitation.[29] In this study, we present a comprehensive photoluminescence analysis of a CZTS solar cell using pulsed laser excitation.

The PL measurements were performed on a Mo/CZTS/CdS/i-ZnO/ITO solar cell based on a spin-coated CZTS absorber fabricated in ambient air from DMSO-based precursors, which exhibited a power conversion efficiency of ~8.4%. Mo-coated soda lime glass was used as a substrate. Post-annealing of the complete devices was conducted in air on hotplate at 300 °C for 12 min using a graphite box. The thickness of the CZTS layer in the solar cell was around 800 nm. Detailed fabrication procedures are provided in Ref. 30. The room-temperature bandgap energy of CZTS, determined from the external quantum efficiency (EQE) spectra, was found to be $E_g = 1.42$ eV and the Urbach energy $E_U = 38.4$ meV. The reduction in bandgap from 1.53 to 1.42 eV observed after post-annealing was attributed to Cd diffusion into the CZTS absorber layer.[30] The temperature dependence of E_g for CZTS was previously measured in Ref. 31. It was demonstrated that there is a 24 meV difference between the E_g values at 300 and 8 K.

Temperature-dependent photoluminescence measurements were carried out by mounting the CZTS solar cell on the cold finger of a closed-cycle helium cryostat (Janis CCS-150). The sample temperature was subsequently reduced to 8 K and controlled up to 300 K using a LakeShore Model 335 temperature controller. For pulsed excitation, the second harmonic (532 nm) of a pulsed Q-switched Nd:YAG laser (CryLaS FQSS266-Q2) was used, operating at 10 kHz with a peak energy of 1.1 μJ, pulse width <1 ns, and a maximum average power (P_{max}) of 7.5 mW. The excitation intensity was adjusted using neutral density filters, and the laser spot size on the sample was approximately 1 mm. This configuration was employed to prevent the solar cell from overheating and damage. The second harmonics of Cobolt 08-DPL Nd:YAG laser operating at 532 nm was used to provide CW PL excitation. CW laser maximum average power was $P_{max} = 10$ mW. The resulting luminescence was filtered through a cutoff low-pass filter and then directed toward a computer-controlled single grating (600 lines mm^{-1}) monochromator (f = 0.64 m) (Horiba Jobin Yvon FHR640). The PL signal was detected using an R632 photomultiplier tube and processed via a DSP Lock-in amplifier (SR810).

Figure 1(a) shows how our CZTS solar cell's PL emission changes with temperature. A single broad asymmetric PL band is observed. The peak position at $T = 8$K is 1.27 eV. Unfortunately, all PL spectra were disturbed by a strong absorption band from water vapor at $E = 1.315$ eV (943 nm). The blue shift of the PL band occurs as the temperature rises. The shape of this band was tested with different asymmetric spectral shapes to get the best fitting result. Among all the tested functions, the ADS profile provided the best fit. An example of this fitting is presented in Fig. 1(b) for the $T = 100$ K spectrum. The ADS shape is given by

$$I(h\nu) = A\left[1\Big/\left(1+\exp\left(-\frac{h\nu-E_1}{W_1}\right)\right)\right] \times\left[1-1\Big/\left(1+\exp\left(-\frac{h\nu-E_2}{W_2}\right)\right)\right], \quad (1)$$

where A, E_1, E_2, W_1, and W_2 are fitting parameters. E_1 and W_1 describe the low-energy side of the band whereas E_2 and W_2 are associated with the high-energy one. PL band parameters I_{max}, E_{max}, and the full width at half maximum (*FWHM*) were calculated using numerical methods. The *FWHM* value ~180 meV did not change with increasing temperature. This is somewhat surprising because usually the FWHM will increase with temperature in CZTS. The relatively constant FWHM at different temperatures shows that the PL band is not caused by typical band-to-defect, band-to-band, or band-to-tail recombinations. The dash-dotted curve in Fig. 1(b) shows a PL spectrum measured with a CW laser at 100 K from the same solar cell. This PL band displays a red shift with increasing temperature that is typical for band-to-defect or band-to-tail recombination in CZTS at lower temperatures.[32,33] It can be seen that the peak position of the CW PL band has a maximum at lower energy, and the half-width of this band is smaller. These results provide evidence that pulsed laser excitation can, in fact, expose extra recombination processes that are not visible with CW lasers. Numerous earlier investigations have demonstrated that the density of states function largely determines the shape of the PL bands in kesterites. Because of exponential band tails, the low energy side of PL bands typically has an exponential shape. However, the situation can be more complicated when both spatial potential fluctuations and bandgap fluctuations are present. We anticipate slightly different PL band shapes when using pulsed lasers because the occupation of various localized states also depends on excitation intensity. In an experiment where all variables remain constant except for the type of excitation, under otherwise identical experimental conditions, pulsed excitation generates approximately 15 times more electron–hole pairs. The population of different localized states exhibits a nonlinear relationship with laser power, resulting in pronounced disparities between continuous wave and pulsed laser sources.[28,29] Even very shallow localized states are occupied by pulsed excitation, which modifies the PL bands' shape. Therefore, the ADS shape of PL bands can indeed indicate changes in the distribution of localized states.

Figure 2(a) shows that the PL band exhibits a continuous blue shift of 78 meV as the temperature increases from 8 to 300 K. This blue shift with increasing temperature is very common in CZTS (when using a CW laser excitation) and can be explained using the

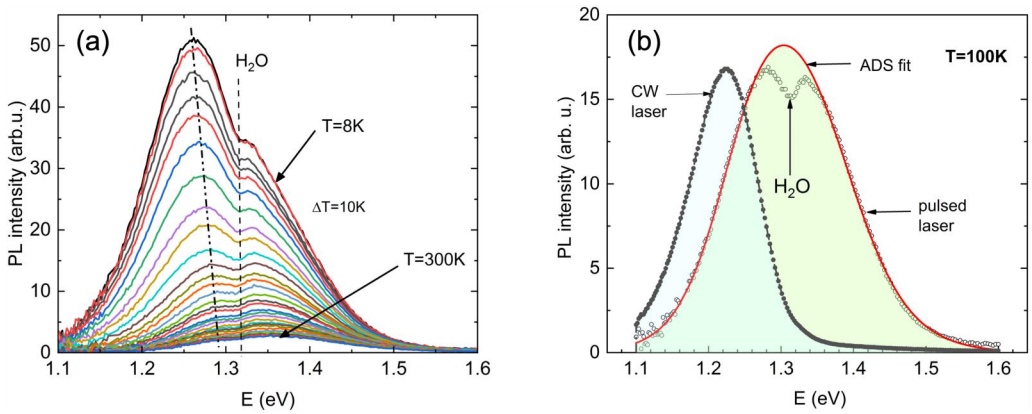

FIG. 1. (a) Photoluminescence (PL) spectra of the CZTS solar cell measured at various temperatures. (b) Red line shows a fitting result of the PL spectrum obtained with pulsed laser at T = 100 K using an ADS profile [Eq. (1)]. The water vapor absorption band at 1.315 eV is indicated by an arrow, and the PL spectrum obtained using a continuous wave (CW) laser is shown as a black dash-dotted curve.

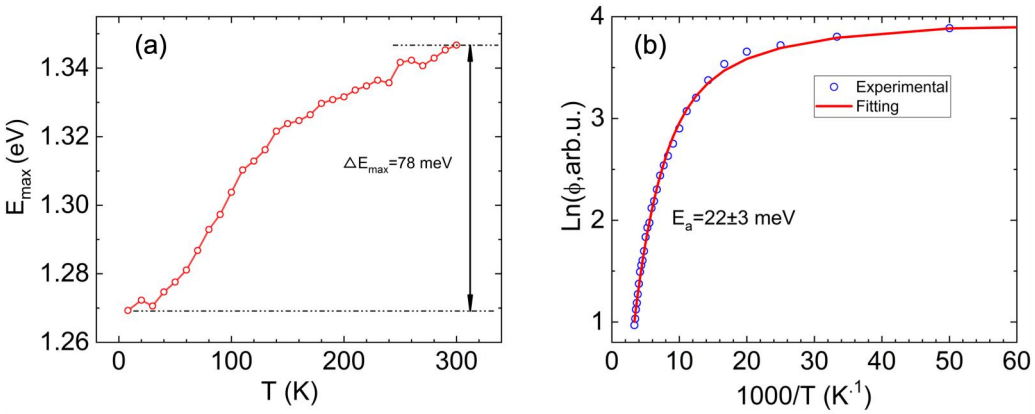

FIG. 2. Temperature dependence of (a) peak position and (b) integrated intensity of PL band. Solid line in (b) is a result of fitting with Eq. (2).

potential fluctuation model, where the energy shift of the PL peak depends strongly on the density and depth of the tail states in the CZTS samples. However, this blue shift typically does not exceed 30–40 meV[34] and can be observed starting at T ≈ 60–100 K while the low-temperature section usually shows a red shift.[35] Therefore, our CZTS sample's notable blue shift of 78 meV suggests that the pulsed laser excitation reveals a very different recombination channel.

According to theory,[18] this type of blue shift is expected and is associated with a process known as tail-to-impurity (TI) recombination at high excitation levels, in which the valence and conduction bands are curved, forming extremely deep localized states for electrons and blocking the passage of holes to these localized electrons. Deep localized states for electrons inside potential wells thus act like deep donors. Strong and quick electron funneling into these potential wells is most likely the reason why our solar cell does not exhibit the often-seen band-to-acceptor or band-to-tail recombination when CW lasers are used for PL excitation. These deep wells may be created by point-like donor clusters, the CdS/CZTS heterojunction, or grain boundaries, which bend the valence and conduction bands locally downward. Grain boundaries could be the most likely source of band bending, even though the volumetric proportion of grain boundary areas is rather low when compared to the total luminous volume. However, we cannot rule out the possibility that the band bending and recombination happen in the heterojunction region. Holes lack the energy necessary to approach potential wells and fill acceptor levels close to the band-bending region at low temperatures. As the temperature increases, more holes can tunnel through the potential barrier and are captured by vacant acceptor levels, leading to the formation of deep donor–deep acceptor pairs. In addition, there is a strong correlation between the occupation of these acceptor levels of donor–acceptor pairs and the distance r from the conduction band wells; that is, the energy levels of closer acceptors are deeper, and the corresponding PL band peak position is at a higher energy. Holes tunneling through the potential barrier and occupying deeper acceptor levels are responsible for the observed blue shift as the temperature increases. A similar blue shift has been reported in $CuGaTe_2$ single crystals,[24,36] GaAs:Si diodes,[37] and in $CH_3NH_3PbBr_3$ perovskite quantum dots.[38]

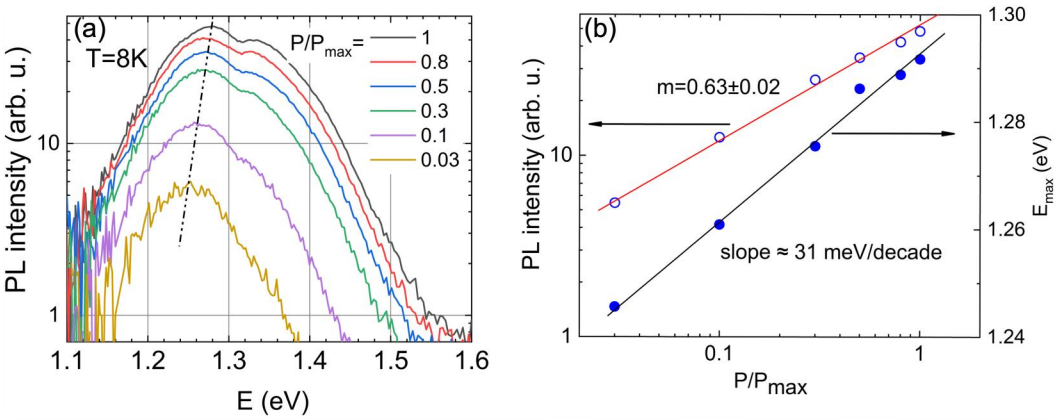

FIG. 3. Excitation power dependence on CZTS cells. PL was measured at $T = 8$ K using a pulsed laser (a); the intensity of the PL band as a function of the laser power was plotted on a log–log scale. The line is the least squares fit to the data; the peak position shift with laser power (b).

The thermal activation energy of the PL band was derived from the Arrhenius plot [Fig. 2(b)], where a theoretical expression for discrete energy levels was used to fit the dependence of ln Φ (T) vs 1000/T,[39]

$$\phi(\mathrm{T}) = \phi_0 / \left[1 + \mathrm{A_1 T^{3/2}} + \mathrm{A_2 T^{3/2}} \exp(-\mathrm{E_a}/\mathrm{kT})\right], \qquad (2)$$

where Φ is an integrated intensity of the PL band, A_1 and A_2 are the process rate parameters, and E_a is the thermal activation energy. The activation energy $E_a = 22$ meV is very low for such a deep PL band. At $T = 8$ K, the energy difference between E_{max} and E_g is 172 meV. The low E_a value may indicate that the relatively deep acceptor level is pushed toward the valence band when holes approach localized electrons, like in the case of the deep donor–deep acceptor (DD–DA) pairs model.[40–42] It is known that when paired with a donor (acceptor) defect, the acceptor (donor) level tends to move closer to the valence (conduction) band because of the Coulombic interaction. In our case, the acceptor level is pushed toward the valence band due to the Coulomb term $\Delta E = e^2/4\pi\varepsilon_0\varepsilon(0)r$. Here, r is the distance between the acceptor defect and the potential well filled with electrons, ε is a static dielectric constant. ΔE has a value of 0.262 eV for lattice constant $a = 0.5434$ nm and 0.132 eV for lattice constant $c = 1.0838$ nm, respectively.[42] Consequently, it is anticipated that the acceptor level of the DD–DA complex with the shortest distance between the donor and the acceptor will be located nearer the valence band edge than for complexes with greater distances. Cu_{Zn} is the most likely deep acceptor defect, and it has been identified in numerous previous studies.[6] These results suggest the presence of very closely spaced DD–DA pairs due to low-temperature quenching activation energy. Shallow acceptor levels of $E_a \sim 30$ meV in CZTS have been previously reported in some papers, though.[6,43]

Figure 3(a) shows that the peak position of the PL band measured at $T = 8$ K also exhibits a discernible blue shift as the laser power increases. As shown in Fig. 3(b), the PL band shifts at a rate of 31 meV per decade of laser power. The strong blue shift of the peak position with increasing laser power is characteristic of so-called heavily doped semiconductors. However, most studies report blue shift values around 15 meV per decade of laser power in CZTS.[33,44–47] Since the DD–DA model typically predicts no blue shift for extremely near donor–acceptor pairings,[41,42] it is unable to explain a significantly larger blue shift in our solar cells. Owing to the extremely high excitation density of the pulsed laser, the so-called band-filling effect is most likely the source of the observed blue shift. The PL spectra's shape did not drastically change as the laser power was increased, and the simple power law of the form $I_{max} \propto P^m$, where I_{max} is the PL band intensity, P is the average laser excitation power, and m is a dimensionless exponent, can be used to fit the experimental data. It is well known that for an excitation laser photon with an energy exceeding the bandgap energy, the coefficient m is generally $1 < m < 2$ for the free- and bound-exciton emission and $m \leqq 1$ for defect-related recombination.[48] The PL band correlates with recombination involving intrinsic defects, as indicated by a m value of 0.63 [refer to Fig. 3(b)].

Figure 4 illustrates the recombination model for the photoluminescence band. It is well known that CZTS thin film exhibits a high concentration of grain boundaries. Therefore, we believe that the PL band could be associated with recombination processes caused by

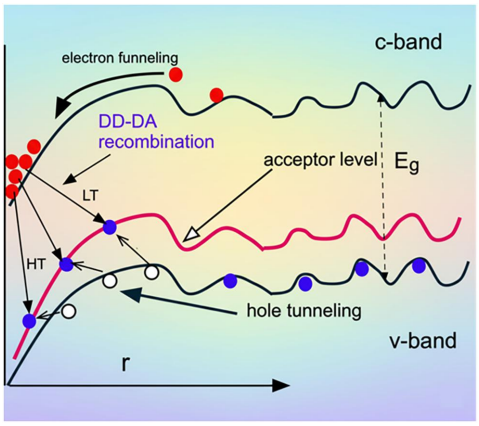

FIG. 4. Recombination model for PL band in CZTS, linked to band bending near grain boundaries or clusters of donor defects. LT and HT represent low and high temperature, respectively.

band bending near these grain boundaries, donor-defect clusters, or the heterojunction. Further studies are needed to identify the exact recombination mechanism. Pulsed laser excitation enables the observation of new PL properties of CZTS absorbers. This advancement opens exciting possibilities for enhancing the efficiency of solar cells. Further investigation into these properties could lead to optimized materials with enhanced energy conversion.

In conclusion, we performed a photoluminescence study of a CZTS thin-film solar cell over the temperature range of 8–300 K using pulsed laser excitation. The PL spectra revealed a single asymmetric band at 1.27 eV (at 8 K) well-fitted with an ADS profile. This band exhibited a blue shift of approximately 0.26 meV/K with increasing temperature. The temperature dependence of the integrated intensity indicated a low activation energy around 22 meV, suggesting recombination involving closely spaced donor–acceptor pairs. Laser power-dependent measurements at 8 K showed that the PL band was shifted by about 31 meV per decade of laser power. The behavior of the PL band was associated with recombination processes near the band-bending region, where the emission energy is sensitive to the acceptor's proximity to these areas. This study demonstrates that high-power pulsed laser excitation enables the observation of novel PL characteristics in CZTS absorber layers.

This work was supported by the European Union through the European Regional Development Fund (Project TK210) and the Estonian Research Council (Grant No. PRG1023). The research was carried out using the NAMUR+ core facility, funded by the Estonian Research Council (TARISTU24-TK26 "Centre of Nanomaterials Technologies and Research").

AUTHOR DECLARATIONS

Conflict of Interest

The authors have no conflicts to disclose.

Author Contributions

Jüri Krustok: Writing – original draft (equal). **Achmad Nasyori:** Investigation (equal); Methodology (equal). **Reelika Kaupmees:** Data curation (equal); Investigation (equal); Writing – review & editing (equal). **Marit Kauk-Kuusik:** Data curation (equal); Funding acquisition (equal); Investigation (equal); Supervision (equal); Writing – review & editing (equal).

DATA AVAILABILITY

The data that support the findings of this study are available from the corresponding author upon reasonable request.

REFERENCES

[1]M. Kauk-Kuusik, K. Timmo, K. Muska, M. Pilvet, J. Krustok, M. Danilson, V. Mikli, R. Josepson, and M. Grossberg-Kuusk, J. Phys. Energy **4**, 024007 (2022).
[2]A. Wang, J. Cong, S. Zhou, J. Huang, J. Cao, X. Cui, X. Yuan, Y. Yao, Z. Xu, G. He, J. Z. Liu, J. M. Cairney, Y. Chen, M. A. Green, S.-H. Wei, K. Sun, and X. Hao, Nat. Energy **10**, 255 (2025).
[3]M. Abbas, S. Chen, Z. Li, M. Ishaq, Z. Zheng, J. Hu, Z. Su, Y. Li, L. Ding, and G. Liang, Nano-Micro Lett. **17**, 257 (2025).
[4]Y. Zhao, X. Chen, S. Chen, Z. Zheng, Z. Su, H. Ma, X. Zhang, and G. Liang, Adv. Mater. **37**, 2409327 (2025).
[5]T. Wu, S. Chen, Z. Su, Z. Wang, P. Luo, Z. Zheng, J. Luo, H. Ma, X. Zhang, and G. Liang, Nat. Energy **10**, 630 (2025).
[6]M. Grossberg, J. Krustok, C. J. Hages, D. M. Bishop, O. Gunawan, R. Scheer, S. M. Lyam, H. Hempel, S. Levcenco, and T. Unold, J. Phys. Energy **1**, 044002 (2019).
[7]T. Raadik, J. Krustok, M. Kauk-Kuusik, K. Timmo, M. Grossberg, K. Ernits, and J. Bleuse, Physica B **508**, 47 (2017).
[8]M. Grossberg, J. Krustok, T. Raadik, M. Kauk-Kuusik, and J. Raudoja, Curr. Appl. Phys. **14**, 1424 (2014).
[9]B. G. Mendis, A. A. Taylor, M. Guennou, D. M. Berg, M. Arasimowicz, S. Ahmed, H. Deligianni, and P. J. Dale, Sol. Energy Mater. Sol. Cells **174**, 65 (2018).
[10]H. Ma, Q. Zhu, L. Zou, B. Xu, H. Wang, R. Ge, F. Yue, Y. Zhang, L. Sun, Y. Chen, and J. Chu, Adv. Energy Mater. **15**, 2405033 (2025).
[11]J. P. Leitão, N. M. Santos, P. A. Fernandes, P. M. P. Salomé, A. F. da Cunha, J. C. González, G. M. Ribeiro, and F. M. Matinaga, Phys. Rev. B **84**, 024120 (2011).
[12]J. J. S. S. Scragg, J. K. Larsen, M. Kumar, C. Persson, J. Sendler, S. Siebentritt, and C. Platzer Björkman, Phys. Status Solidi B **253**, 247 (2016).
[13]W. Chen, D. Dahliah, G.-M. Rignanese, and G. Hautier, Energy Environ. Sci. **14**, 3567 (2021).
[14]J. K. Larsen, J. J. S. Scragg, N. Ross, and C. Platzer-Björkman, ACS Appl. Energy Mater. **3**, 7520 (2020).
[15]J. J. S. Scragg, L. Choubrac, A. Lafond, T. Ericson, and C. Platzer-Björkman, Appl. Phys. Lett. **104**, 041911 (2014).
[16]J. Bleuse, F. Ducroquet, and H. Mariette, J. Electron. Mater. **47**, 4282 (2018).
[17]S. Siebentritt, N. Papathanasiou, and M. C. Lux-Steiner, Physica B **376–377**, 831 (2006).
[18]A. P. Levanyuk and V. V. Osipov, Sov. Phys. Usp. **24**, 187 (1981).
[19]J. Krustok, H. Collan, M. Yakushev, and K. Hjelt, Phys. Scr. **T79**, 179 (1999).
[20]M. Grossberg, J. Krustok, J. Raudoja, K. Timmo, M. Altosaar, and T. Raadik, Thin Solid Films **519**, 7403 (2011).
[21]M. Grossberg, J. Krustok, J. Raudoja, and T. Raadik, Appl. Phys. Lett. **101**, 102102 (2012).
[22]S. Chen, J.-H. Yang, X. G. Gong, A. Walsh, and S.-H. Wei, Phys. Rev. B **81**, 245204 (2010).
[23]M. Grossberg, T. Raadik, J. Raudoja, and J. Krustok, Curr. Appl. Phys **14**, 447 (2014).
[24]J. Krustok, J. Raudoja, M. Yakushev, R. D. Pilkington, and H. Collan, J. Appl. Phys. **86**, 5305 (1999).
[25]M. Kauk-Kuusik, K. Timmo, K. Muska, M. Pilvet, J. Krustok, R. Josepson, G. Brammertz, B. Vermang, M. Danilson, and M. Grossberg, ACS Appl. Energy Mater. **4**, 12374 (2021).
[26]J. Li, J. Huang, Y. Huang, H. Tampo, T. Sakurai, C. Chen, K. Sun, C. Yan, X. Cui, Y. Mai, and X. Hao, Sol. RRL **5**(10), 2100418 (2021).
[27]M. Gansukh, Z. Li, M. E. Rodriguez, S. Engberg, F. M. A. Martinho, S. L. Mariño, E. Stamate, J. Schou, O. Hansen, and S. Canulescu, Sci. Rep. **10**, 18388 (2020).
[28]J. A. Smyder, A. R. Amori, M. Y. Odoi, H. A. Stern, J. J. Peterson, and T. D. Krauss, Phys. Chem. Chem. Phys. **16**, 25723 (2014).
[29]J. Krustok, J. Kokla, R. Kaupmees, M. Grossberg-Kuusk, and M. Kauk-Kuusik, J. Phys. Energy **7**, 035003 (2025).
[30]A. Nasyori, M. Pilvet, A. Saar, J. Krustok, M. Danilson, R. Kaupmees, V. Mikli, Y. Gong, R. Josepson, E. Saucedo, M. Grossberg-Kuusk, and M. Kauk-Kuusik, J. Mater. Chem. A **13**, 30167 (2025).
[31]W. Li, K. Jiang, J. Zhang, X. Chen, Z. Hu, S. Chen, L. Sun, and J. Chu, Phys. Chem. Chem. Phys. **14**, 9936 (2012).
[32]İ. Mengü, K. Muska, M. Pilvet, V. Mikli, E. Dudutienė, R. Kondrotas, J. Krustok, M. Kauk-Kuusik, and M. Grossberg-Kuusk, Sol. Energy Mater. Sol. Cells **277**, 113124 (2024).
[33]J. Krustok, R. Kaupmees, N. Abbasi, K. Muska, I. Mengü, and K. Timmo, Phys. Status Solidi RRL **17**(9), 2300077 (2023).
[34]L. Q. Phuong, M. Okano, Y. Yamada, A. Nagaoka, K. Yoshino, and Y. Kanemitsu, Appl. Phys. Lett. **104**, 081907 (2014).
[35]J. P. Teixeira, R. A. Sousa, M. G. Sousa, A. F. da Cunha, P. A. Fernandes, P. M. P. Salomé, and J. P. Leitão, Phys. Rev. B **90**, 235202 (2014).

[36]A. Jagomägi, J. Krustok, M. Grossberg, M. Danilson, and J. Raudoja, Phys. Status Solidi **203**, 949 (2006).
[37]S. H. Park and B. D. Choe, J. Appl. Phys. **68**, 5916 (1990).
[38]H. C. Woo, J. W. Choi, J. Shin, S. H. Chin, M. H. Ann, and C. L. Lee, J. Phys. Chem. Lett. **9**, 4066 (2018).
[39]J. Krustok, H. Collan, and K. Hjelt, J. Appl. Phys. **81**, 1442 (1997).
[40]J. Krustok, H. Collan, K. Hjelt, J. Mädasson, and V. Valdna, J. Lumin. **72–74**, 103 (1997).
[41]J. Krustok, J. Raudoja, M. Krunks, H. Mändar, and H. Collan, J. Appl. Phys. **88**, 205 (2000).
[42]J. Krustok, T. Raadik, M. Grossberg, M. Kauk-Kuusik, V. Trifiletti, and S. Binetti, Mater. Sci. Semicond. Process. **80**, 52 (2018).
[43]K. Hönes, E. Zscherpel, J. Scragg, and S. Siebentritt, Physica B **404**, 4949 (2009).
[44]L. Yin, G. Cheng, Y. Feng, Z. Li, C. Yang, and X. Xiao, RSC Adv. **5**, 40369 (2015).
[45]D. Tiwari, M. V. Yakushev, T. Koehler, M. Cattelan, N. Fox, R. W. Martin, R. Klenk, and D. J. Férmin, ACS Appl. Energy Mater. **5**, 3933 (2022).
[46]S. Campbell, Y. Qu, J. D. Major, D. Lagarde, C. Labbé, P. Maiello, V. Barrioz, N. S. Beattie, and G. Zoppi, J. Phys. D **52**, 135102 (2019).
[47]T. M. Ng, M. T. Weller, G. P. Kissling, L. M. Peter, P. Dale, F. Babbe, J. de Wild, B. Wenger, H. J. Snaith, and D. Lane, J. Mater. Chem. A **5**, 1192 (2017).
[48]T. Schmidt, K. Lischka, and W. Zulehner, Phys. Rev. B **45**, 8989 (1992).